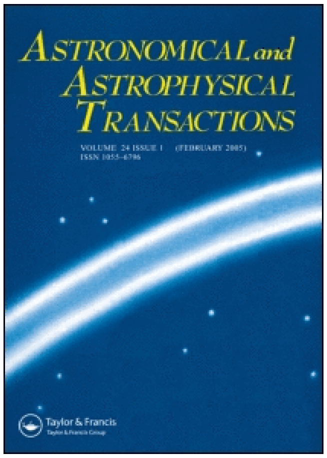

Astronomical & Astrophysical Transactions
The Journal of the Eurasian Astronomical Society
Publication details, including instructions for authors and subscription information:
http://www.informaworld.com/smpp/title~content=t713453505

The broad emission lines in the active galactic nucleus Fairall 9

L. S. Nazarova [a]; N. G. Bochkarev [b]; P. T. O'brien [c]
[a] Euro-Asian Astronomical Society, Moscow, Russia
[b] Sternberg Astronomical Institute, Moscow State University, Moscow, Russia
[c] Department of Physics and Astronomy, University of Leicester, Leicester, UK

Online Publication Date: 01 August 2007
To cite this Article: Nazarova, L. S., Bochkarev, N. G. and O'brien, P. T. (2007) 'The broad emission lines in the active galactic nucleus Fairall 9', Astronomical & Astrophysical Transactions, 26:4, 401 - 408
To link to this article: DOI: 10.1080/10556790701685615
URL: http://dx.doi.org/10.1080/10556790701685615

Astronomical and Astrophysical Transactions
Vol. 26, Nos. 4–5, August–October 2007, 401–408

Taylor & Francis
Taylor & Francis Group

The broad emission lines in the active galactic nucleus Fairall 9

L. S. NAZAROVA*†, N. G. BOCHKAREV‡ and P. T. O'BRIEN§

†Euro-Asian Astronomical Society, 13 Universitetskij Prospect, Moscow 119992, Russia
‡Sternberg Astronomical Institute, Moscow State University, 13 Universitetskij Prospect, Moscow 119992, Russia
§Department of Physics and Astronomy, University of Leicester, Leicester, LE1 7RH, UK

(Received 12 January 2007)

This paper reports on a study of UV and optical spectra of the active galaxy Fairall 9 taken as a part of the International AGN Watch database. CIV/Lyα, Lyα/Hß and Hα/Hß ratios have been measured at different radial velocities, which are varied across the line profiles. The ratio Lyα/Hß is low in the low-velocity centre of the lines, but increases a little in the high-velocity wings. The CIV/Lα and Hα/Hß line intensities ratios, however, are high at the line centre but become low in the wings. Modelling with the photoionization code CLOUDY shows that the observed line ratios can be described by two systems of clouds. One corresponds to the high-ionization line zone (HIL) with an electron density, $n_e \sim 10^{8-10}$ cm^{-3}. It is presumably located above the accretion disk or in the jets. The other system corresponds to the low-ionization line zone (LIL), which is probably a part of the accretion disk and which has a higher electron density, $n_e \sim 10^{12-13}$ cm^{-3}. The possible geometry of the BLR in Fairall 9 is discussed.

Keywords: Active galactic nuclei; Seyfert galaxies; Broad line regions; Photoionization modelling

1. Introduction

High temporal frequency monitoring of Seyfert galaxies (AGN Watch programme) over an extended period has proved to be a powerful way to understand the structure and the physical conditions of the broad line region (BLR). The shape of broad emission line profiles varies within the same object, depending on the ionization level of the species producing the line. It was shown that BLR in the active galactic nuclei (AGN) has a complex structure, with the observed line emission being a sum of the contribution each part. The accretion disk emission should be in most BLR of active galaxies according to the data available today. The double-peaked emission lines are often used as a strong indication of the disk presence [1–3]. However, the optical and UV lines show a dramatic difference between the double-peaked Balmer and single peaked UV line profiles. The different shapes of the optical and UV lines also indicate the existence of two or more line-emitting regions [4–6].

*Corresponding author. Email: ludmila@kzn.ru

Astronomical and Astrophysical Transactions
ISSN 1055-6796 print/ISSN 1476-3540 online
http://www.tandf.co.uk/journals
DOI: 10.1080/10556790701685615

A clue to the problem can lie in a detailed study of the physical conditions along the line profiles together with line profile variations, since it provides an insight into the distance between the black hole and the emission region, if different parts of the line profiles are produced at a different distances from the centre. To this purpose we have examined the variability along the line profiles of the Lα, CIV, Hß and Hα in Fairall 9, using available results of simultaneous UV and optical observations obtained during an extensive monitoring in the framework of AGN Watch program.

The paper is organized as follows. The observational data using for this study are described in section 2; the results of the analysis of the line profiles given in section 3; the photoionization modelling of the line ratios are presented in section 4 and the summary is given in section 5.

2. Observational data

The UV and optical spectra of Fairall 9 were taken from the AGN Watch database for the period May 1994–January 1995 (in correspondence with papers [7, 8]). We have chosen four UV and six optical spectra at dates close to moments of maximal and minimal Fairall 9 nucleus luminosity during the taken period. Details of these spectra are given in table 1.

Figure 1 shows the continuum light curve at $\lambda = 1390$ Å, taken from AGN Watch database (see [7, 8]). The spectral distribution of the central continuum of Fairall 9 is taken from [9].

3. Analysis of the line profiles

The profiles of the high ionization lines Lα and C IV 1550 Å near the maximum and the minimum of Fairall 9 continuum light curve are presented on figure 2 together with the difference of that fluxes. The Lα and C IV 1550 Å profiles look similar especially at the minimum of the nucleus activity. Zheng and O'Brien [11] noticed that the profiles of these lines as well as Mg II 2800 Å line are quite similar at the minimum. However, they found the consistent increase of the Lα line width with the incident flux level, with a FWHM variation from $\sim$2500 to 3800 km s^{-1}. They also found that the major change in C IV 1550 Å line took place near the line centre, but with an extension towards the blue wing centred about -2500 km s^{-1}. In our study the differences of the line intensities at maximum and at minimum of continuum flux (figure 2) show an additional emission at blue wing near -2000 km s^{-1} in both Lα and CIV lines.

The profiles at maximum and at minimum of the low ionization lines Hα and Hß together with the difference of the fluxes are presented in figure 3. The line profile Hß shows the blue

Table 1. Log of spectroscopic observations.

Date	JD (2449000+)	Lines
1994 May 10	482.672	Lyα, C IV 1550 Å
1994 May 18	490.676	Lyα, C IV 1550 Å
1994 Oct 27	653.492	Lyα, C IV 1550 Å
1994 Nov 08	665.191	Lyα, C IV 1550 Å
1994 May 11	483.933	Hß
1994 May 15	487.922	Hß, Hα
1994 May 19	491.924	Hß
1994 Jun 11	514.846	Hß, Hα
1994 Oct 28	653.739	Hß
1994 Nov 08	664.676	Hß

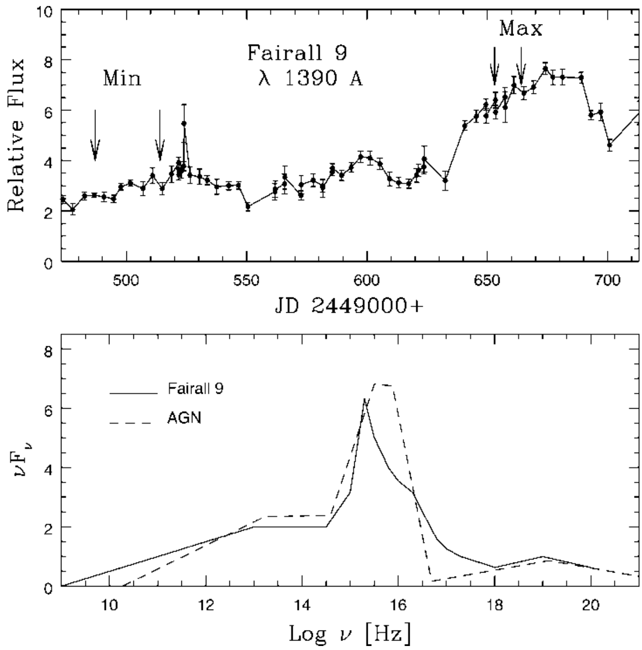

Figure 1. Continuum light curve of Fairall 9 at wavelength $\lambda = 1390$ Å. Arrows indicate the Julian Dates (JDs) of the spectra selected at the minimal and at the maximal states of the nuclear brightness (top). The spectral energy distribution (SED) νF_ν in arbitrary units for Fairall 9 [9] and for the canonical [10] AGN continuum (bottom).

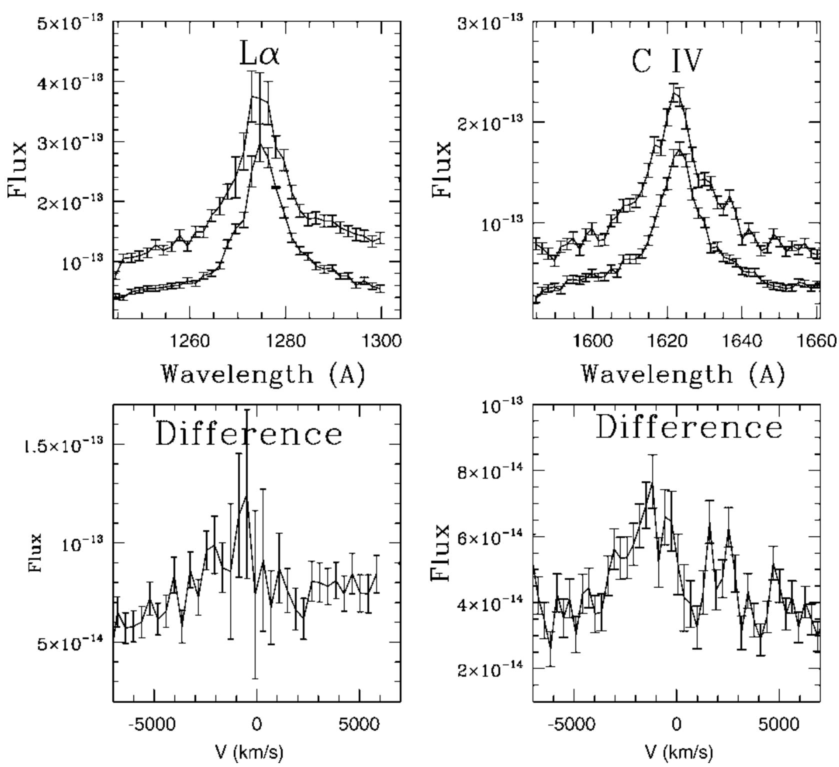

Figure 2. Line profiles of Lα and C IV 1550 Å (top) together with the difference of the fluxes at minimum and at maximum states of nuclear activity of Fairall 9 (bottom). Fluxes are given in erg cm^{-2} s^{-1} Hz^{-1}.

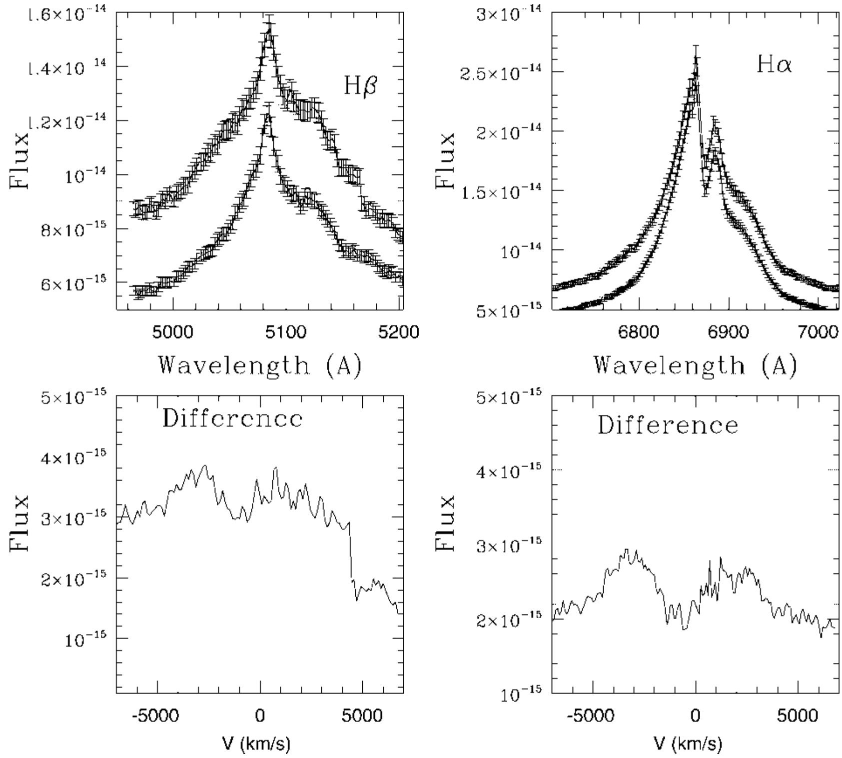

Figure 3. Line profiles of Hß and of Hα (top) together with the difference of the fluxes at minimum and at maximum states of nuclear activity of Fairall 9 (bottom).

and the red bumps which are prominent at the difference of the fluxes. These bumps are located approximately at $\pm 2500\,\mathrm{km\,s^{-1}}$. A similar difference in the fluxes is seen in the Hα line.

Such double peaked structure of the emission lines (figure 3) are usually used as a strong indication of an accretion disk presence [1–4]. However, the difference of the fluxes in the high ionization lines Lyα and C IV 1550 Å do not show a similar structure as in the low ionization lines Hα and Hß (figure 2).

The profiles of the C IV 1550 Å, Lα, Hß and Hα lines have been divided into seven parts, the width of each part being equal to $2000\,\mathrm{km\,s^{-1}}$. The core of the lines is measured between -1000 and $+1000\,\mathrm{km\,s^{-1}}$. Thus, the blue and the red wings have a width of $\pm 7000\,\mathrm{km\,s^{-1}}$. The observed line ratios CIV/Lα, Lα/Hß, and Hα/Hß in the galaxy Fairall 9 are changed differently along the line profiles. The Lα/Hß line ratio is low at the centre of lines but the CIV/Lα and Hα/Hß ratios are high at the centre of lines.

The Hα/Hß line ratio decrease with the increasing intensity of the central source. A similar changes of the Hα/Hß line ratio has been discovered in NGC 5548 Shapovalova *et al.* [12]. Increasing of the CIV/Lα line ratio in Fairall 9 with the increasing the UV continuum (figure 2) was also noticed by Binette *et al.* [13].

4. Photoionization models

The modelling of the observed line ratios CIV/Lα, Lα/Hß and Hα/Hß has been done with the photoionization code CLOUDY (version c9005; Ferland *et al.* [14]), in its plan parallel version, and assuming solar abundances. The assumed spectral distribution of the central continuum is taken from Zheng *et al.* [9] (figure 1).

The computed line ratios CIV/Lα, Lα/Hß and Hα/Hß for given central luminosity as a function of the distance versus the electron density n_e are shown on figure 5. Differing covering factors C are considered for the distributions of the clouds. Three functional dependencies on the distance r have been chosen:

$$C \sim r^{-1}, C = const. \text{ and } C \sim r.$$

From the comparison of the observed (figure 4) and the computed line ratio CIV/L$\alpha \sim$ 0.4–0.8 at minimum and $\sim$ 0.7–1.2 at maximum (figure 5) we can see that the electron density along the lines may change from $10^8\,\text{cm}^{-3}$ to $10^{10}\,\text{cm}^{-3}$. The observed line ratio Lα/Hß $\sim$ 5–20 is small compared to the computed models. Although this line ratio (figure 4) does not show a clear tendency nevertheless the observed line ratio Lα/Hß may corresponds to both cases: a low density $10^{8-9}\,\text{sm}^{-3}$ and a high density $10^{13}\,\text{cm}^{-3}$.

The Hα/Hß ratio is high at the centres of lines (equal to 3–4) and corresponds to the density $10^{11-12}\,\text{cm}^{-3}$ and low (1–2) in the line wings (corresponds to $10^{13}\,\text{cm}^{-3}$). The correction for interstellar absorption was not taken into account because it is small $E_{\text{B-V}} = 0.05$ for Fairall 9.

Thus, these ratios implies that the only way to get this sort of behaviour is if the density is at least about an order of magnitude higher for the gas emitting at higher velocity. This could be accomplished with a density going from $10^{8-10}\,\text{cm}^{-3}$ at low velocity up to $10^{12-13}\,\text{cm}^{-3}$

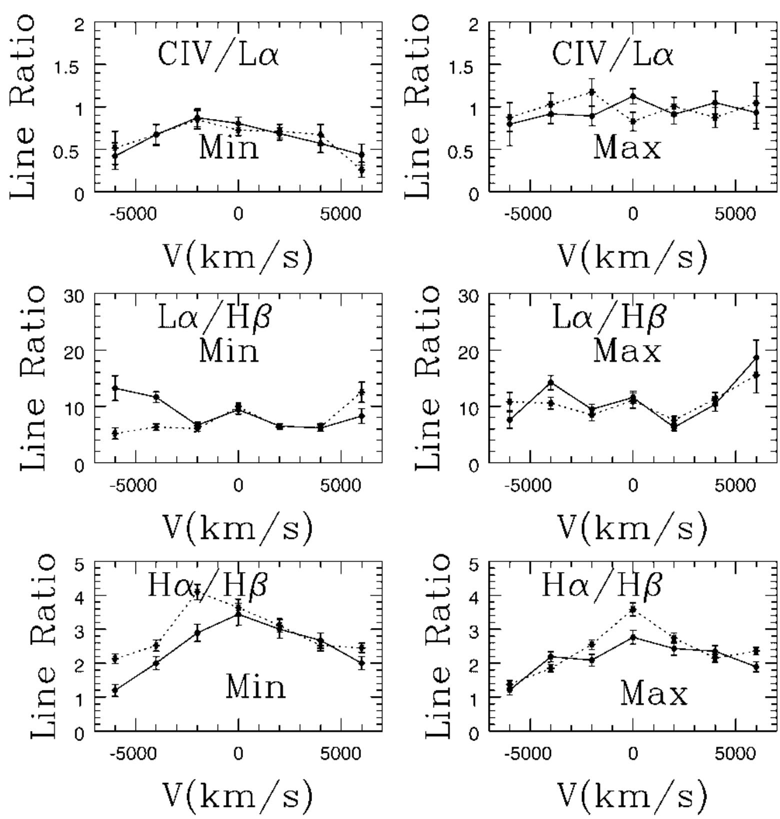

Figure 4. Line ratios CIV/Lα, Lα/Hß and Hα/Hß for the minimal (left side) and for maximal (right side) states of nuclear activity in Fairall 9.

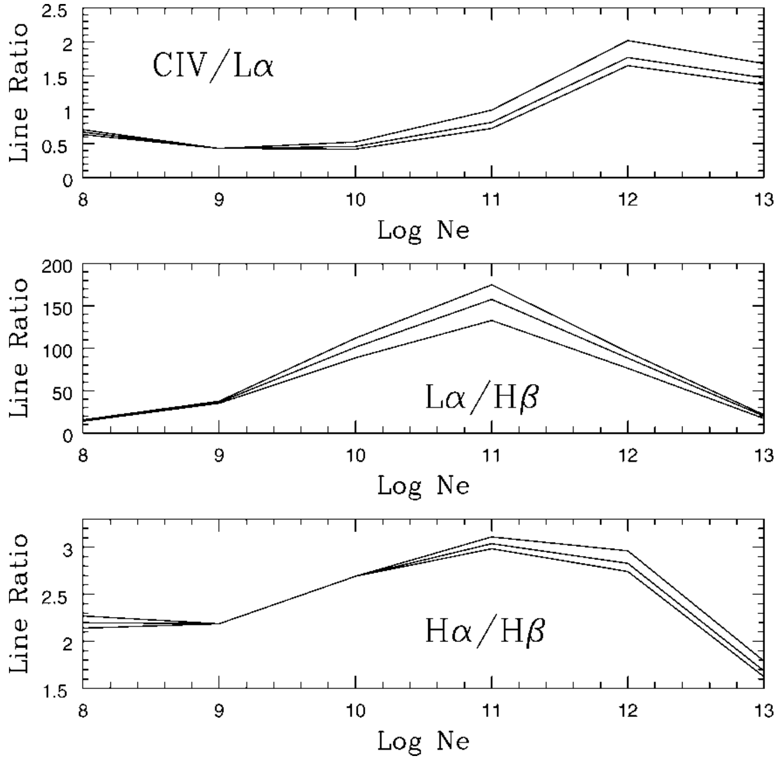

Figure 5. CIV/Lyα, Lyα/Hß, and Hα/Hß line ratios versus electron densities for differing radial dependencies of the covering factor (C). The solid lines correspond to the high state of nuclear activity and the dotted lines to the low state.

at higher velocity. While the CIV/Lα, Lα/Hß and Hα/Hß line ratios show that the electron density is higher in the higher-velocity gas, there is a discrepancy in the actual ranges of density. This is possibly because only a single component has been taken to represent two different cloud components. The different density ranges implied by the variation of line ratio with velocity can be reconciled, however, if we have two components, a low ionization line (LIL) zone and a high ionization line (HIL) zone.

Let us accept that the electron density obtained from the ratio of the high ionization lines CIV/Lα corresponds to the HIL zone located above an accretion disk (possibly in jets) with the electron densities $n_e \sim 10^{8-10}\,\mathrm{cm}^{-3}$, while the LIL zone located in accretion disk has the electron density $n_e \sim 10^{12-13}\,\mathrm{cm}^{-3}$ obtained from low ionization line ratio Hα/Hß. This model supports the analysis of the flux difference in high and low ionization lines (figures 2 and 3). The flux difference in low ionization lines Hα and Hß shows the double peaked structure, which is characterized by the possible presence an accretion disk, but similar flux differences in the high ionization lines have only a blue peak and could be localized in the jet.

It is interesting to notice that Zheng and O'Brien [11], when studying UV lines variability in Fairall 9 also found that the BLR region in Fairall 9 has a complex structure, possibly with non-spherical components.

The line ratios for two intensities of the central continuum are shown in figure 6. Comparison of the observed (figure 4) and computed (figure 6) line ratios for different intensities of central source shows that the observed line ratio Lα/Hß at high and at low states is nearly the same. The observed Hα/Hß line ratio decreases slightly in the high state of the central continuum. This effect coincides with the predicted changing of the line ratio with increasing intensity of the

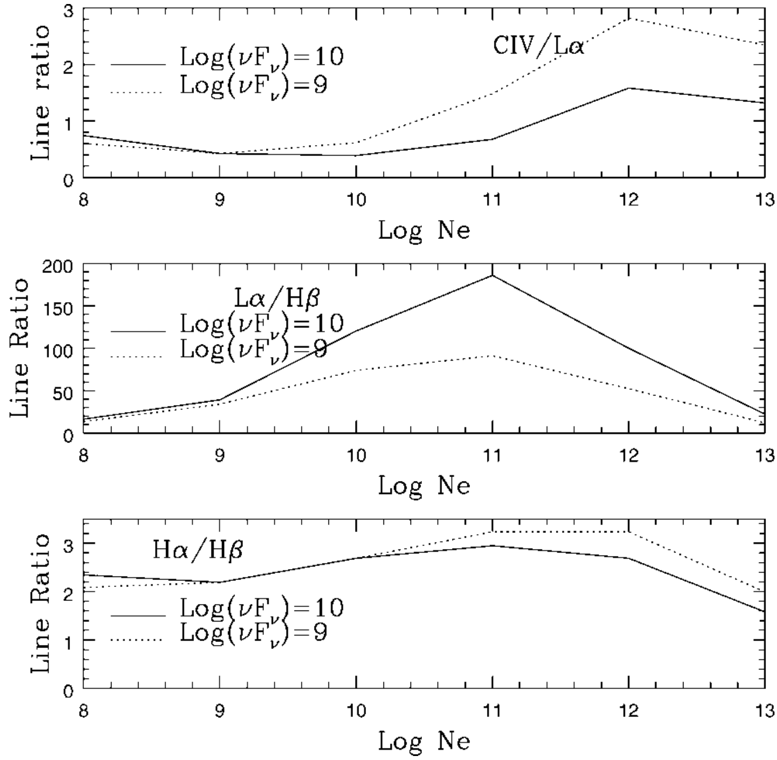

Figure 6. The CIV/Lyα, Lyα/Hß and Hα/Hß line ratios versus electron densities for the differing intensities of the central continuum.

central source (figure 6). However, the observed CIV/Lα line ratio contradicts the theoretical prediction. The observed line ratio CIV/Lα is higher in the high state but the theoretical ratio decreases in the high state. This disagreement has been discussed by Binette *et al.* [13] and Netzer [15]. They suggest that the broad emission lines may be ionized by a two-component continuum. Binette *et al.* [13] suggest that two independently variable continuum components (a primary optical to UV component, and a secondary X-ray component) are anisotropic, whereas the secondary and UV components are isotropic. Netzer [15] suggested that the optical-UV component is anisotropic, whereas the secondary X-ray component is isotropic. Our study suggests that there are two emission regions with different electron densities and different localizations: an accretion disk (with high density $10^{12-13}\,\mathrm{cm}^{-3}$) and jets (with low density gas $10^{8-10}\,\mathrm{cm}^{-3}$). Most of the high ionization lines are formed in the low density regions $n_e \sim 10^{8-10}\,\mathrm{cm}^{-3}$ where the theoretical line ratio CIV/Lyα is nearly independent of the increasing of the central continuum. Therefore, the increasing intensity of the central continuum leads to no change or only a small increase in the CIV/Lα line ratio.

5. Conclusions

The broad line regions in Fairall 9 could be represented by a two-component model:

1. The electron density obtained from the ratio of the high ionization lines CIV/Lα corresponds to the HIL zone located above an accretion disk (possibly in jets) with the electron densities $n_e \sim 10^{8-10}\,\mathrm{cm}^{-3}$.

2. The electron density obtained from the ratio of the low ionization line Hα/Hß corresponds to the LIL zone located in an accretion disk with the electron density $n_e \sim 10^{12-13}$ cm^{-3}.

The components have different localizations, densities, and contributions to the line profiles.

Acknowledgements

This research has been partially supported by RFBR grant 06-02-16843.

References

[1] K. Chen, J.P. Halpern and A.V. Filippenko, Astrophys. J. **339** 742 (1989).
[2] K. Chen and J.P. Halpern, Astrophys. J. **344** 115 (1989).
[3] M. Eracleous and J.P. Halpern, Astrophys. J. Suppl. Ser. **90** 1 (1994).
[4] M. Eracleous, J.P. Halpern and J.C. Charlton, Astrophys. J. **582** 633 (2003).
[5] S.A. Snedden and C.M. Gaskell, Bull. AAS **36** 732 (2004).
[6] L.S. Nazarova, N.G. Bochkarev and C.M. Gaskell, Aston. Astrophys. Trans. **23** 343 (2004).
[7] P.M. Rodriguez-Pascual, D. Alloin, J. Clavel *et al.*, Astrophys. J. Suppl. Ser. **110** 9 (1997).
[8] M. Santos-Lleo, E. Chatzichristou, C. Mendes de Oliveira *et al.*, Astrophys. J. Suppl. Ser. **112** 271 (1997).
[9] W. Zheng, G.A. Kriss, A.F. Davidsen and J.W. Kruk, Astrophys. J. **454** L11 (1995).
[10] W.G. Matthews and G.J. Ferland, Astrophys. J. **323** 456 (1987).
[11] W. Zheng and P.T. O'Brien, Astrophys. J. **356** 463 (1990).
[12] A.I. Shapovalova, V.T. Doroshenko, N.G. Bochkarev *et al.*, Astron. Astrophys. **422** 925 (2004).
[13] L. Binette, A. Prieto, E. Szuzkiewicz and W. Zheng, Astrophys. J. **343** 135 (1989).
[14] G.J. Ferland *et al.*, University of Kentucky, Department of Physics and Astronomy, Internal Report (2004).
[15] H. Netzer, Mon. Not. R.A.S. **225** 55 (1987).